

PN fast winds: Temporal structure and stellar rotation

R. K. Prinja^{1*}, D.L. Massa², M. A. Urbaneja³, R.-P. Kudritzki³

¹*Dept. of Physics & Astronomy, University College London, Gower Street, London WC1E 6BT*

²*Space Telescope Science Institute, 3700 San Martin Drive, Baltimore, MD 21218, USA*

³*Institute for Astronomy, University of Hawaii, 2680 Woodlawn Drive, Honolulu, HI 96822, USA*

Accepted 2009. Received 2009; in original form 2009

ABSTRACT

To diagnose the time-variable structure in the fast winds of PN central stars (CSPN), we present an analysis of P Cygni line profiles in *FUSE* satellite far-UV spectroscopic data. Archival spectra are retrieved to form time-series datasets for the H-rich CSPN NGC 6826, IC 418, IC 2149, IC 4593 and NGC 6543. Despite limitations due to the fragmented sampling of the time-series, we demonstrate that in all 5 CSPN the UV resonance lines are variable primarily due to the occurrence of blueward migrating discrete absorption components (DACs). Empirical (SEI) line-synthesis modelling is used to determine the range of fluctuations in radial optical depth, which are assigned to the temporal changes in large-scale wind structures. We argue that DACs are common in CSPN winds, and their empirical properties are akin to those of similar structures seen in the absorption troughs of massive OB stars. Constraints on PN central star rotation velocities are derived from Fast-Fourier Transform analysis of photospheric lines for our target stars. Favouring the causal role of co-rotating interaction regions, we explore connections between normalised DAC accelerations and rotation rates of PN central stars and O stars. The comparative properties suggest that the same physical mechanism is acting to generate large-scale structure in the line-driven winds in the two different settings.

Key words: stars: mass-loss – stars: evolution – stars: rotation – ultraviolet: stars

1 INTRODUCTION AND BACKGROUND

The central stars of planetary nebulae (CSPN) mark a critical stage in the evolution of low to intermediate mass stars, and thus the majority of stars in our Galaxy. Of significant interest are the fast winds evident in young H-rich (O-star type) CSPN, through which $\sim 10^{-8}$ to $10^{-6} M_{\odot} \text{ yr}^{-1}$ of mass can be driven off the star, and with wind terminal velocities of up to a few 1000s km s^{-1} (e.g. Kudritzki, Urbaneja & Puls, 2006, and references therein). Accurate knowledge of the fast stellar winds is important for understanding the evolution of CSPN and for decoding their spectral diagnostics. Mass loss from CSPN is also a key process in the interacting stellar wind (ISW) model that may explain some of the PN morphologies observed (e.g. Balick & Hajain 2004). Stellar binarity could also have a pivotal role in shaping non-spherical nebulae (see e.g. De Marco 2009) and central star binarity represents a useful potential laboratory for examining asymmetric wind phenomenon. In this respect PNs can contribute to our knowledge of analogous settings such

as Wolf-Rayet nebulae, luminous blue variables (LBVs) and Galactic Centre phenomena.

Our focus in this paper is to explore similarities between the fast wind properties of H-rich CSPN and the radiation pressure driven winds of luminous OB stars, and in particular the evidence for inhomogeneities and structure in the winds. *International Ultraviolet Explorer (IUE)* spectroscopy of OB star winds has revealed widespread variability seen primarily in the blueward extended absorption troughs of resonance line doublets (e.g. Massa et al. 1995; Kaper et al. 1997; Prinja et al. 2002). Several case studies have demonstrated that the UV line profile fluctuations in massive, luminous stars are due to evolving (over days), organised structures in the wind, which may have a physical origin rooted to the stellar surface (e.g. Fullerton et al. 1997; de Jong et al. 2001). The presence of structure and wind clumping affects mass-loss rates derived from different spectral diagnostics (e.g. Sundqvist, Puls & Feldmeier 2010; Prinja & Massa 2010) and the resultant wind porosity can complicate significantly the radiative forcing used in theoretical mass loss rate determinations (e.g. Muijres et al. 2011). The fast winds of H-rich CSPN provide a laboratory for constraining the origin of wind structure and comparisons

* E-mail: rkp@star.ucl.ac.uk (RKP)

to massive star outflows. The CSPN offer unique tests for the role of radiative instabilities, large scale structures, and stellar rotation over a wide range of critical length scales. For example the rotation period (for fixed projected rotation velocity) and wind flow time (for fixed terminal velocity) both scale as stellar radius, and are therefore reduced in CSPN relative to normal OB stars. Our present study of structure in CSPN fast winds also has potential relevance to studies of variable features on the stellar surface that then propagate into the wind, such as the sub-surface convection zones studied by Cantiello et al. (2009).

The identification and characterization of variable wind structure in hot stars demands time-series spectroscopy of diagnostic spectral lines, over an appropriately extended time-scale and with sufficiently intensive monitoring. The *Far Ultraviolet Spectroscopic Explorer (FUSE)* time-series of NGC 6543 studied by Prinja et al. (2007) is the most suitable dataset currently available in the UV archives for the analysis of large-scale wind structure in CSPN. Their analysis revealed clear evidence for recurrent discrete absorption components (DACs) in NGC 6543 akin to the features commonly seen in several OB stars. We aim in the present paper to place the findings of Prinja et al. (2007) on a wider observational footing and we present here a survey of *FUSE* time-series datasets of CSPN. We extract the time-variable FUV characteristics of NGC 6826, IC 418, IC 4593 and IC 2149. An additional archival dataset of NGC 6543 (to the fuller one presented by Prinja et al. 2007) is also included here. Other UV archives such *IUE* and *HST* do not currently contain any additional high-resolution time-series datasets of H-rich CSPN that are appropriate for studying variable wind structure.

In the following sections we introduce the *FUSE* time-series samples and present an analysis of temporal features in the Doppler-shifted absorption troughs. Velocity measurements are supplemented by radial optical depths derived from empirical SEI (Sobolev with Exact Integration; Lamers et al. 1997; Massa et al. 2003) line synthesis modelling of the P ν $\lambda\lambda$ 1118, 1128 resonance doublet. The determination of fundamental parameters is extended to include estimates of the projected rotation velocity of the 5 target central stars using the fast Fourier transform (FFT) technique.

2 THE *FUSE* TIME-SERIES SAMPLE

Our CSPN sample is derived from archival *FUSE* data available via the NASA Multimission Archive at Space Telescope (MAST). We initially searched for *FUSE* observations in the object category 70 (‘Planetary Nebula and central star’). The ~ 200 spectra listed were then narrowed to H-rich (O-type) stars that had at least one unsaturated, but well-developed P Cygni line profile in the *FUSE* range. From these data we only retained those objects that had at least 4 sequential observations available within a span of 12 hours; this was deemed a minimum requirement to permit an inspection for the incidence of organised wind structure features in the line profiles. These criteria reduced the available sample to the 5 H-rich CSPN listed in Table 1. (The epoch of the dataset of NGC 6543 included here predates the time-series presented by Prinja et al. 2007.) The datasets were secured using either the LWRs ($30'' \times 30''$) or MDRS

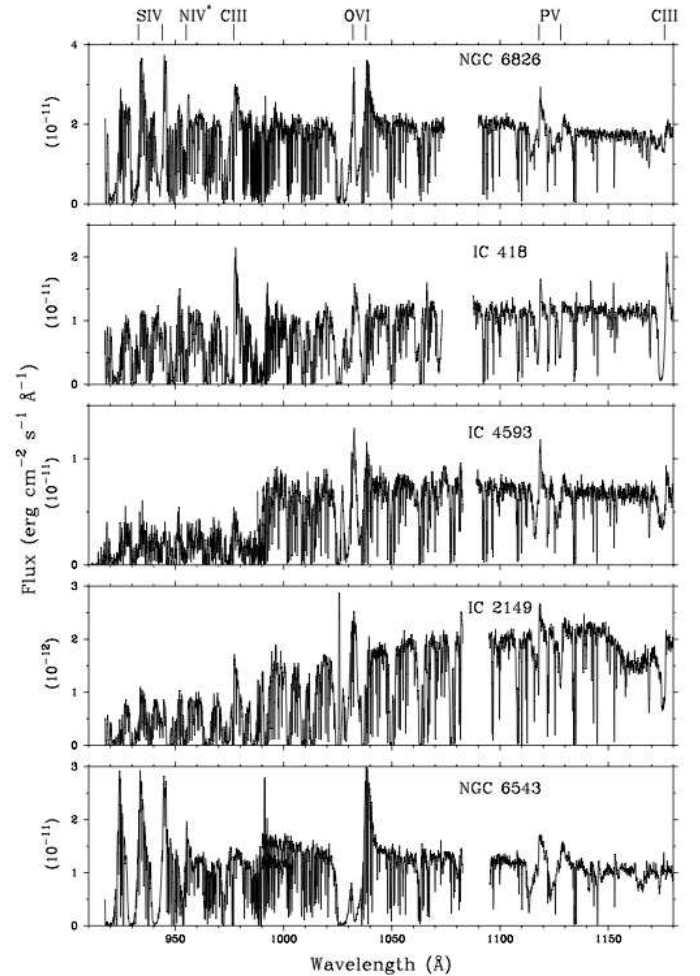


Figure 1. Mean *FUSE* spectra for the 5 CSPN stars examined for wind variability; key wind-formed line of interest are marked.

($4'' \times 20''$) spectrograph apertures (Table 1). In all cases, except IC 2149, the data were recorded in HIST mode, with individual exposure times between ~ 7 to 8 minutes. The time-series of IC 2149 is based on temporal segments obtained in time-tagged event lists (TTAG mode), with a total exposure of 21910 sec. The individual spectra were aligned using strong interstellar lines to account for wavelength drifts in the *FUSE* non-guide channels. The data studied here were gridded to a resolution of 0.1\AA and the mean spectrum for the *FUSE* channels available are shown in Fig. 1. Adopted fundamental stellar parameters based on published non-LTE model atmosphere analyses are collated in Table 1.

The typical continuum signal-to-noise of an individual *FUSE* spectrum is only ~ 15 and at this quality the most suitable spectral line for a study of variable wind structure is the P ν $\lambda\lambda$ 1118, 1128 resonance line doublet. The P ν line is unsaturated and its doublet separation of $\sim 2690 \text{ km s}^{-1}$ is large enough compared to the typical terminal velocity, v_∞ of our targets such that the each component is reasonably well resolved, thus helping to remove ambiguities in the occurrence of optical depth and velocity structure in limited time-series datasets.

All five targets listed in Table 1 have been previously documented by Handler (2003) as exhibiting semi-regular

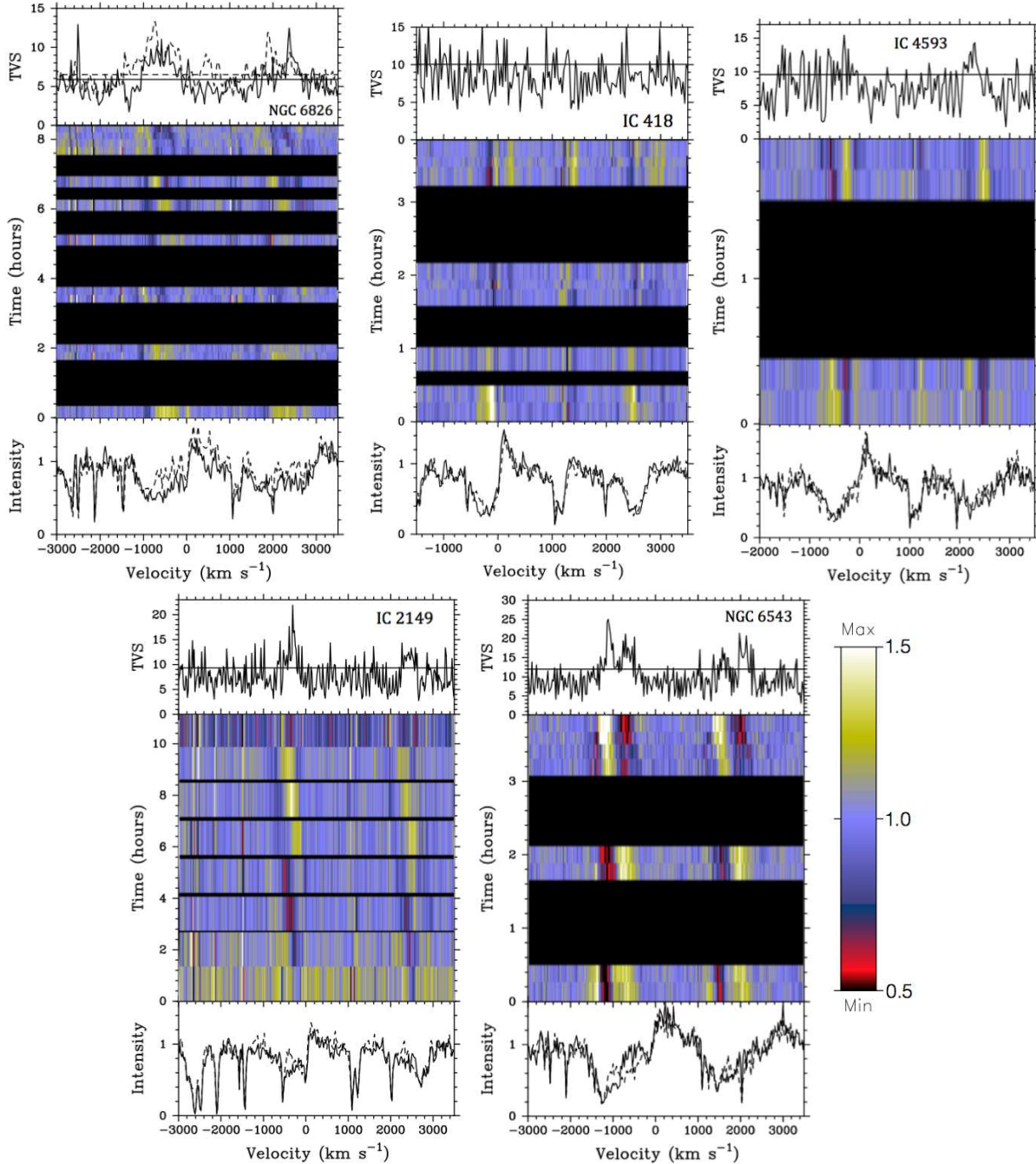


Figure 2. Dynamic spectra showing the evidence for structure in P v $\lambda\lambda$ 1117.98, 1128.01 in the winds of PN central stars: Clockwise from the top-left, NGC 6826, IC 418, IC 4593, NGC 6543 and IC 2149. For each case, the upper panel displays the temporal variance spectrum (TVS) and 95% confidence limit (horizontal lines). The panels below the dynamic spectra show pairs of the variable P v line profiles. In the case of NGC 6826 the TVS for an additional dataset from 2007 January is also shown (dashed line).

photometric variability, over time-scales ranging from ~ 3.5 to 6.5 hours. Handler (2003) proposes that these stars form part of a class of variable objects labelled ZZ Leoparis stars, where the prototype is the central star of IC 418 (HD 35914). Previously, pairs of high-resolution *IUE* spectra of our target stars secured more than a year apart revealed mostly tentative evidence for changes in the blue-ward wings of saturated P Cygni profiles (e.g. Patriarchi & Perinotto, 1995,

1997). We present here analyses of organised, and temporal, stellar wind structure in this sample of H-rich CSPN.

2.1 Optical spectra

High resolution ($R=68000$) optical spectra of the stars in our sample were collected with the echelle spectrograph ES-PaDONs at the 3.6-m Canada-France-Hawai'i telescope in

the summit of Mauna Kea during the spring of 2008, under excellent weather conditions. The collected data were processed with the data reduction package Libre-ESPRIT (Donati et al. 1997). The extracted spectra cover almost entirely the 3700–10500Å wavelength range, with a signal-to-noise ratio in the continuum above 200, except for the very blue end of the observed range. In the following, we will use the optical spectra to complement our FUV series in order to estimate the rotational velocities of our stars.

3 DISCRETE ABSORPTION COMPONENTS

Inspection of the line profiles in the *FUSE* fragmented time-series datasets listed in Table 1 suggests that all five target CSPN have outflows that vary on hourly timescales. The fluctuations are mostly at the ~ 10 to 15% of the continuum level and over a substantial portion of the absorption trough in PV, CIII and OVI. Corresponding changes are seen in different line species, which is more consistent with a notion of line-of-sight density changes rather than extreme ionization shifts.

Following a well established approach, dynamic spectra (colour-scale images) of the time-series data of each CSPN are presented in Fig. 2. Ratios of individual PV $\lambda\lambda 1118, 1128$ line profiles divided by the mean for the time-series are used to highlight the variability present. For each dynamic spectrum in Fig. 2, the uppermost-panel shows the temporal variance spectrum, TVS (see e.g. Fullerton et al. 1996), and the corresponding bottom panel exhibits pairs of PV line profiles to illustrate the typical intensity changes. The TVS estimates the significance of the line profile variability as a function of velocity. Not only do the central stars reveal \sim hourly variability in the fast wind, the evidence in Fig. 2 is that the changes are primarily in the form of blue-ward migrating features, closely matching in empirical appearance the discrete absorption components (DACs) that are commonly seen in the UV spectra of OB stars (see Sect. 1). We note also the ubiquity of the variability in CSPN such that whenever the spectral diagnostics and data are available, variability is detected. The results in Fig. 2 indicate wind changes occurring at very low velocities (less than 100 km s⁻¹) in some of the time-series, which (as in OB stars) suggests a causal connection to deep-seated structure at or close to the stellar surface. Brief summaries of the DACs in each CSPN follow below:

NGC 6826 – We identify the occurrence of two sequential DACs over ~ 8.5 hours. The first feature is seen already formed at the start of the time-series at ~ -450 km s⁻¹ and migrates to ~ -1000 km s⁻¹ over about 4 hours. The second DAC is evident immediately after the data gap between ~ 4 to 5 hours in Fig. 2. This second feature drifts from ~ -250 km s⁻¹ to ~ -900 km s⁻¹ over ~ 3.5 hours.

IC 418 – Despite the sparse dataset, and with the caveat that the variability is weak, we identify one DAC-like feature in IC 418. It progresses from ~ -250 km s⁻¹ at the start of the observations and has shifted to ~ -350 km s⁻¹ over the subsequent 2 hours.

IC 4593 – This is the most limited *FUSE* dataset for our sample of stars, with only 4 spectra spanning about 2 hours. Nevertheless there is evidence from the well separated PV doublets of temporal structure in the absorp-

tion trough. We identify in Fig. 2 a feature that travels from ~ -200 km s⁻¹ to ~ -500 km s⁻¹. In this case, and in IC 418 above, confidence in this detection comes from the fact that corresponding structures are seen in both components of the PV doublet, and that similar behaviour is evident in for example CIII $\lambda 1176$.

IC 2149 – One well monitored DAC is present in PV profiles of this central star. Using eight exposures, we trace its progression from ~ -100 km s⁻¹ to almost ~ -500 km s⁻¹ over ~ 11 hours.

NGC 6543 – Prinja et al. (2007) have already demonstrated that NGC 6543 exhibits recurrent DACs in its wind-formed FUV lines, using *FUSE* data secured in 2007 January. We show here (Fig. 2) that two successive features are also present in data taken more than 5 years earlier. The phenomenon is therefore clearly long lived in CSPN, as in the case for DACs in individual luminous OB stars.

Guided by the dynamic spectra in Fig. 2, the central velocities of discrete absorption components were estimated using by-eye cursor values for each individual spectrum; the poor signal-to-noise of the spectra precludes the use of any more sophisticated approach (such as Gaussian fitting). We estimate that the DAC central velocities quoted have errors of ± 50 km s⁻¹. The velocities for individual DAC episodes in our sample are plotted in Fig. 3 (left-hand panel) as a function of time. Linear fits to these data yield accelerations which range between $\sim 1.0 \times 10^{-2}$ km s⁻² to 5.3×10^{-2} km s⁻². The accelerations (a_{DAC}) are listed in Table 3.

In the well monitored cases of NGC 6826, IC 2149 and NGC 6543 a key characteristic of the DACs is that both their propagation and recurrence time-scales (of \sim few hours) are longer than the characteristic wind flow time, R_*/v_∞ (\sim less than 1 hr). The same relative comparison of timescales is commonly noted for DACs evolving in the winds of OB stars and has led to the conclusion in massive star studies that the large-scale structures mostly arise due to perturbations, such as velocity plateaus, in the stellar wind (see e.g. the hydrodynamical simulations of Lobel & Blomme, 2008). Further comparisons of CSPN and O star DAC accelerations is postponed to Sect. 6.

4 MEASUREMENTS FROM EMPIRICAL LINE-SYNTHESIS FITTING

We seek in this section to derive additional empirical measures that reflect the variability of the CSPN fast winds, with the underlying premise of Sect. 2 that the line profile changes are principally due to the actions of DAC-like features. Our approach is described in Prinja et al. (2007) and relies on matching the PV doublet lines with model profiles generated using a modified version the SEI methods of Lamers, Cerruti-Sola & Perinotto (1987). The primary difference in the SEI code used here has been documented by Massa et al. (2003) and the modification is motivated by the need to reproduce UV line profiles where the absorption troughs are not smooth, but affected by localised optical depth structure. Aside from all the standard parameterisations in the SEI code (e.g. velocity law and macro-turbulence), the radial optical depth, $\tau_{\text{rad}}(w)$, is obtained from the fits by varying 21 independent velocity bins, each $\sim 0.05 v_\infty$ wide. This approach affords greater flexibility in matching the absorption

Table 1. Fundamental central star parameters.

CSPN	Sp.type	$v \sin i$ (km/s)	Distance (pc)	T_{eff} (kK)	$\log g$ (cgs)	L_*/L_{\odot}	He abund.	Ref.
NGC 6826	Of (H-rich)	50	1590	46.0	3.80	4.11	0.10	KUP2006
IC 418	Of (H-rich)	56	1300	36.7	3.55	3.88	0.25	MG2009
IC 4593	Of (H-rich)	55	3225	40.0	3.60	4.04	0.10	KUP2006
IC 2149	Of (H-rich)	54	3258	38.0	3.45	4.45	0.10	U2012
NGC 6543	Of (H-rich)	85	1623	67.0	5.30	3.76	0.10	G2008

References: Kudritzki, Urbaneja & Puls (2006; KUP2006); Morisset & Georgiev (2009; MG2009); Georgiev et al. (2008; G2008); Urbaneja et al. 2012 in preparation (U2012). Distances taken from Stanghellini, Shaw & Villaver (2008), except for IC 418, taken from Guzman et al. (2009). The He abundances are relative to H. The projected rotation velocities ($v \sin i$) are derived in Sect. 5.

Table 2. FUSE fragmented time-series datasets.

CSPN	FUSE Prog.	Aperture	Date	No. of spectra	Total span (hrs)
NGC 6826	P1930401	MDRS	7 Aug. 2000	12	8.5
IC 418	P1151111	LWRS	2 Dec. 2001	9	3.8
IC 4593	B0320102	MDRS	3 Aug. 2001	4	1.9
IC 2149	P1041401	LWRS	2 Dec. 1999	8	11.1
NGC 6543	Q1080202	MDRS	1 Oct. 2001	8	3.7

profile morphology, and in the current application offers a measure of the change in optical depth due to the presence of DACs.

TLUSTY plane-parallel model atmosphere spectra (e.g. Hubeny & Lanz, 1995) were adopted as good approximations for the photospheric contributions underlying the wind-formed PV line profiles in our sample stars. The input photospheric absorption was included as a 'lower boundary' in the SEI models, and we adopted TLUSTY synthesised spectra corresponding closely to the T_{eff} and $\log g$ values listed in Table 1 (and Sect. 5). Individual PV profiles were fitted by varying the 21 $\tau_{\text{rad}}(w)$ bins and an overall measure of the strength of the wind profile is provided by the product of mass-loss rate and P^{4+} ionization fraction ($\dot{M} q(P^{4+})(w)$). Mean $\langle \dot{M} q(P^{4+}) \rangle$ values over $0.2 \leq v/v_{\infty} \leq 0.9$ were determined, assuming solar abundances

We show in Fig. 4 the SEI line synthesis matches obtained for cases of maximum and minimum values of $\langle \dot{M} q(P^{4+}) \rangle$, derived from fitting all the PV profiles in the fragmented time-series of each CSPN. The full range of $\langle \dot{M} q(P^{4+}) \rangle$ values for each central star are listed in Table 3, together with the key SEI velocity law parameters. Even within a short dataset such as IC 418, the $\langle \dot{M} q(P^{4+}) \rangle$ values can differ by a factor of 2 in less than 4 hours. The rest of the stars exhibit $\sim 25\%$ changes in this measure over several hours.

The radial optical depth, $\tau_{\text{rad}}(w)$, determined for each PV spectrum in our sample of CSPN is plotted as function of normalised velocity on the right-hand panels in Fig. 2. The changes in the optical depth arise from variability that is principally due to the occurrence and temporal behaviour of the DACs (e.g. Fig. 2). The optical depth changes are more substantial at low to intermediate velocities (~ 0.2 to $0.5 v_{\infty}$), even in cases where the PV absorption troughs remain reasonably shallow and are sensitive to line profile changes beyond $0.5 v_{\infty}$. The ratio of maximum to minimum radial optical depth measured for each star is listed in Table 3. The $\tau_{\text{rad}}(\text{max})/\tau_{\text{rad}}(\text{min})$ values correspond to specific velocities

where a DAC is present. This ratio rises to between ~ 5 to 10 in our sample. Assuming the line flux changes depend on the optical depth of optically thick large scale wind structures, and forward-scattering is small, the results in Table 3 and Fig. 4 suggest that the DAC features can occult between 10% to 85% of the stellar surface.

5 CSPN ROTATIONAL VELOCITIES

There is a general dearth of published rotation velocity measurements for CSPN. As is typical for hot, high gravity stars, the H and He photospheric lines in CSPN are intrinsically very broad and not ideally suited for determining the projected rotation velocity, $v \sin i$. From the perspective of understanding plausible physical mechanisms for generating large-scale structure in line-driven winds, the parameter space offered by CSPN can be potentially valuable. Stellar evolution calculations predict that single star progenitors of CSPN should be slowly rotating ($V_{\text{eq}} < 1 \text{ km s}^{-1}$; see e.g. Langer et al. 1999; Suijs et al. 2008). Rotation velocity measurements of CSPN can therefore also test the angular momentum transport mechanisms implemented in the evolutionary calculations or alternatively highlight implications for spin up due to binary interactions.

In order to estimate the projected rotational velocities of the stars, we consider a sample of FUV lines that are formed in or near the photosphere of these objects and that our models predict do not show a significant blend with other species, namely O III 1151 and O III 5592. The results derived from these two lines can be validated with several other metal lines, but the specific lines depend on each star, given the range of physical parameters cover by our sample. Therefore, we primarily rely on the two O III lines.

To derive a first estimation, we apply the FFT technique (Gray 1992). When comparing the observed profiles with synthetic ones convolved with the derived rotational rates, it is apparent that rotation alone does not account for all the observed width of the lines. By analogy with re-

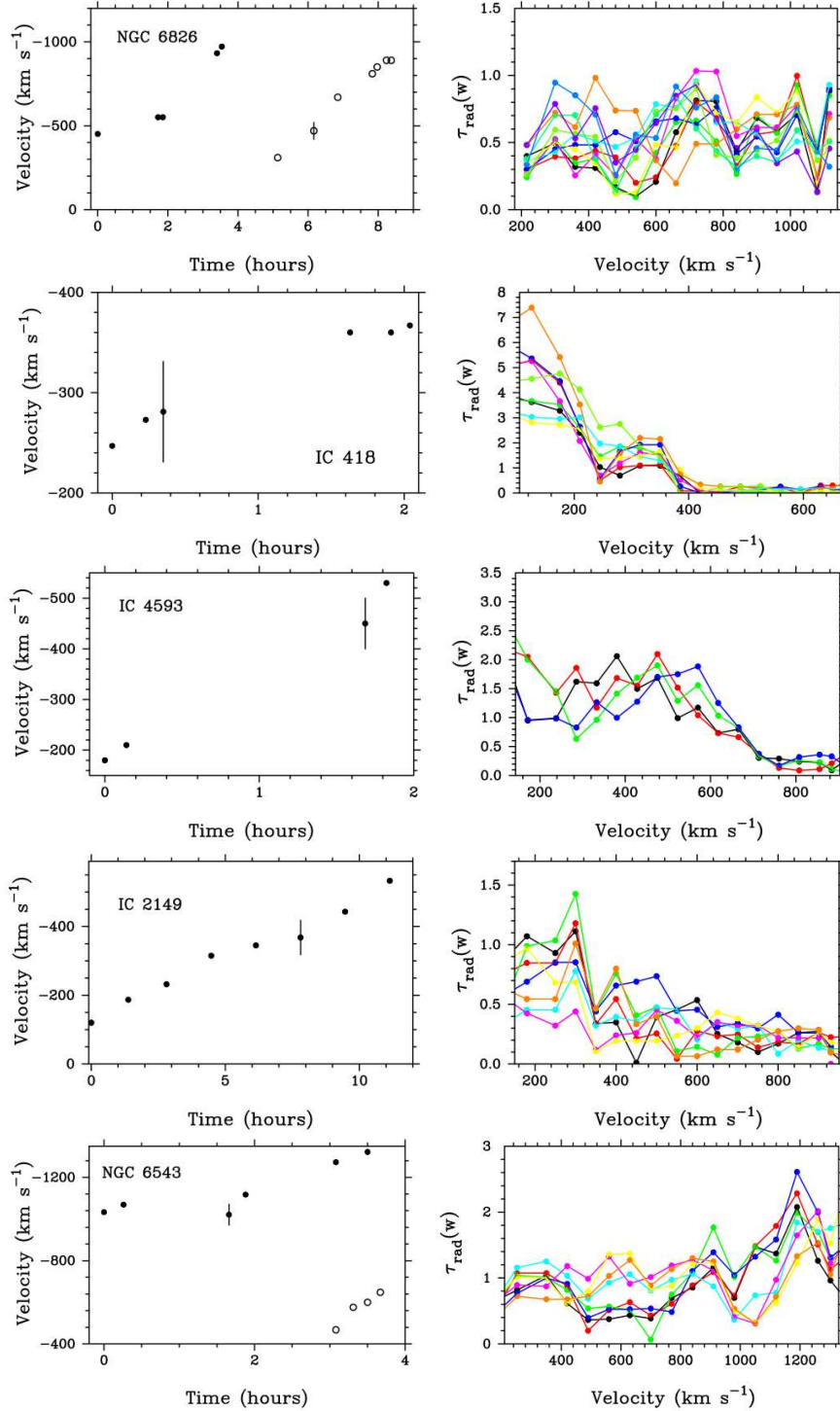


Figure 3. Left-hand panels: The central velocities of migrating discrete absorption components (DACs) as a function of time in the PV doublet profiles of the target CSPN. The corresponding changes in (SEI-derived) radial optical depth (Sect. 4) for the time-series line profiles are shown in the (right-hand panels). We assign an error of $\pm 5\%$ in the $\tau_{\text{rad}}(w)$ values adopted in each velocity bin.

cent work on massive stars (see Simón-Díaz & Herrero 2007 and references therein), we consider that this extra broadening is caused by the presence of a macroturbulent velocity field. While its interpretation is far from clear (although see Aerts et al. 2009 and Simón-Díaz et al. 2010 for interpretations in term of stellar pulsations), it seems that the

consideration of macroturbulence (accounted for in the form of radial-tangential macroturbulence, Gray 1992) improves the profile fits. Hence we apply a method to estimate this extra broadening based on the construction of Gaussian profiles with very narrow full width half maximum and with the same equivalent width as the observed lines. These syn-

Table 3. SEI line-synthesis results.

CSPN	a_{DAC} (km s^{-2})	v_{∞} (km s^{-1})	β	v_{turb}	range $\langle \dot{M} q P^{4+} \rangle$ ($10^{-9} M_{\odot} \text{ yr}^{-1}$)	$\tau_{\text{rad}}(\text{max})/\tau_{\text{rad}}(\text{min})$ [DAC]
NGC 6826	0.053	1200	1.2	0.04	6.7 – 8.9	7.8 (at $0.45 v_{\infty}$)
IC 418	0.016	700	3.0	0.13	3.5 – 6.7	5.7 (at $0.35 v_{\infty}$)
IC 4593	0.042	950	3.0	0.07	14.3 – 16.2	2.9 (at $0.30 v_{\infty}$)
IC 2149	0.009	1000	3.0	0.09	8.5 – 12.3	10.5 (at $0.55 v_{\infty}$)
NGC 6543	0.022	1400	1.0	0.05	4.6 – 5.9	4.8 (at $0.35 v_{\infty}$)

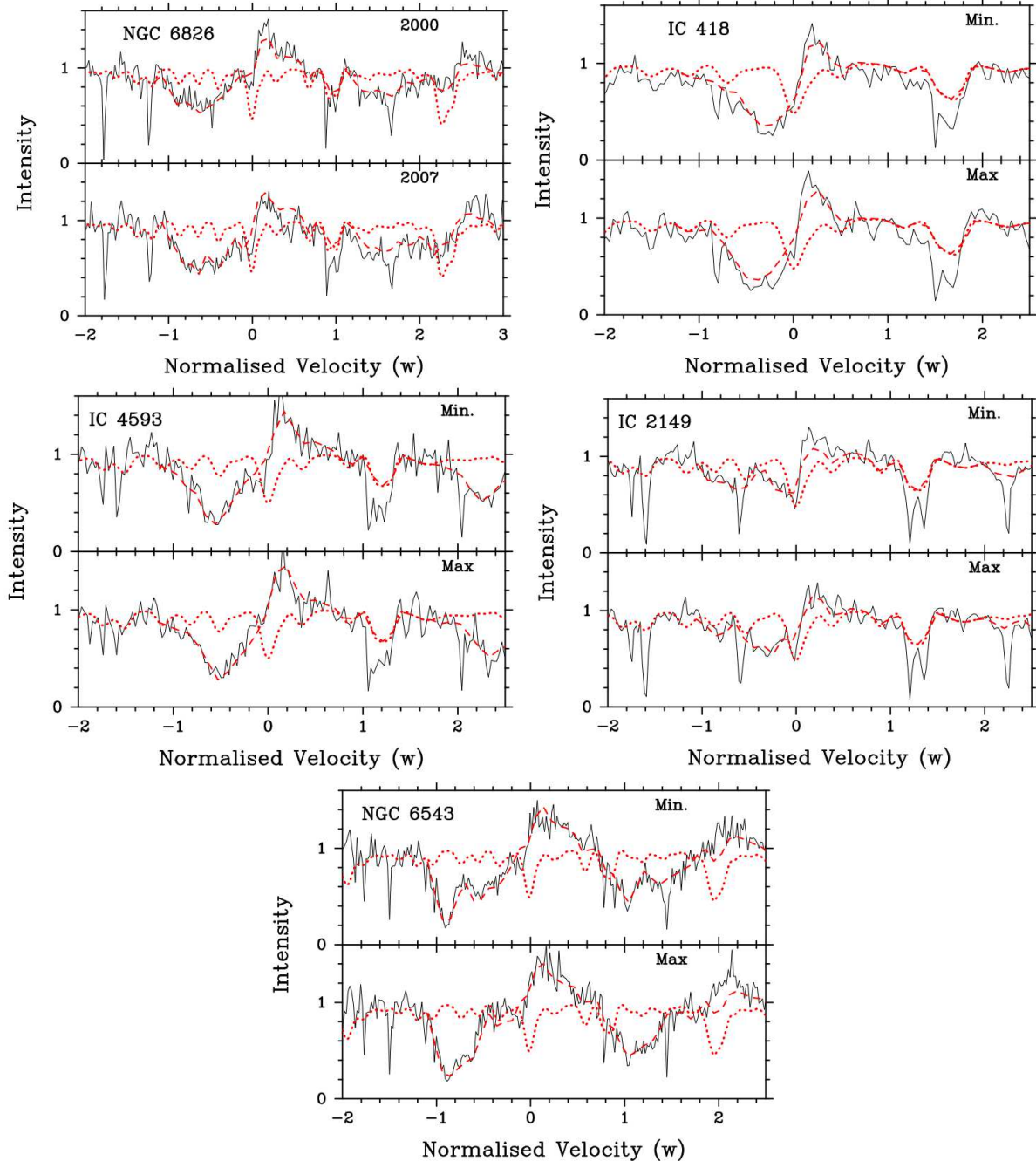


Figure 4. Examples of SEI-line synthesis model profile fits (dashed line) to extreme variability cases in $\text{Pv } \lambda\lambda 1117.98, 1128.01$ for each of the target stars. The adopted TLUSTY photospheric spectrum is also shown in each PN central star case (dotted line). For NGC 6826 an additional extreme case from 2007 January is also matched (e.g. Fig. 2) (Normalised velocity = v/v_{∞}).

thetic lines are first degraded to the spectral resolution of our observed data. The lines are then convolved with the rotational velocities obtained with the FFT method. The best estimate of the extra broadening is then found through a minimization of the residuals between the observed and synthetic profiles convolved with a set of macroturbulent velocities. In general, a marginally improved fit is achieved when a macroturbulence-to- $v_{\text{sin } i}$ ratio of 0.9-1.0 is considered. A representative example of the FFT fit obtained for IC 2149 based on UV and optical spectral lines is shown in Fig. 5

Our finally adopted $v_{\text{sin } i}$ values obtained by means of the FFT technique, are quoted in Table 1. We estimate conservative uncertainties of 10-15 km s⁻¹ in these measurements. The results and parameters listed in Table 1 indicate that the maximum rotation periods for the central stars in our sample range between ~ 0.4 days (NGC 6543) and ~ 2.0 days (IC 418, IC 4593). Note that a substantial evolution in the velocity of the DACs is witnessed during a fraction of the maximum rotation periods, even in the case of NGC 6543.

6 DISCUSSION

In the winds of luminous OB stars, which like CSPN are also radiation pressure-driven, the principal tracer of large-scale wind structure is the incidence of recurrent discrete absorption components (DACs), which migrate blueward across the absorption troughs of extended P Cygni line profiles. The DACs in OB stars have been extensively studied by utilising high-quality UV time-series datasets obtained with the *IUE* satellite (see e.g. Kaper et al. 1997; Massa et al. 1995; Prinja et al. 2002). A key constraint on the origin of DACs comes from evidence that the characteristic timescale for variability in OB star winds is related to the rotation period of the star. The measured acceleration and recurrence timescales of the DACs reveal trends as a function of projected rotation velocity, $v_{\text{sin } i}$, such that faster developing, more frequently recurring DACs are generally apparent in stars with higher $v_{\text{sin } i}$ (e.g. Prinja 1988; Kaper et al. 1997; Prinja et al. 2002). Additionally studies of recombination formed Balmer lines suggest that the cyclical behaviour revealed by the DACs extends down to the inner wind, and possibly to the surface of the star (e.g. de Jong et al. 2001). Subsequent hydrodynamic models showed that coherent wind structures due to co-rotating interaction regions (CIRs) which are linked to structures that are rooted at the stellar surface can at least quantitatively explain the empirical behaviour of the DACs (e.g. Cranmer & Owocki, 1996; Lobel & Blomme 2008).

Our present investigation of PN fast winds has revealed evidence of DACs in *FUSE* P Cygni line profiles of 5 central stars. We conclude that the empirical properties of these features, including central velocity progression, line-of-sight velocity dispersion and recurrence suggest that we are witnessing essentially the same physical phenomenon that is commonly evident in massive stars. Testing relations between DAC time-scales and stellar rotation for CSPNs would require considerably more UV datasets, with adequate sampling at multiple epochs and for stars with a larger range of rotational velocities.

However, it is instructive to examine the normalised (dimensionless) DAC acceleration parameter $a_{\text{DAC}}R_{\star}/v_{\infty}^2$.

This variable would be identically constant if DAC absorption originated in CIRs which were due to material confined to infinitely thin streak lines (Brown et al. 2004). In actuality, the finite extent of the material responsible for DACs causes deviations from such a simple scaling law. Nevertheless, this parameter represents a scaling factor indicative of CIR related motion. We compared the values of this parameter derived here for our sample of CSPN to O star DAC accelerations obtained from Kaper et al. (1999) data for 68 Cygni, ξ Per, λ Cep, ζ Ori A, 19 Cep, λ Ori A, 15 Mon and 10 Lac. The respective accelerations and adopted parameters are listed in Table 4. For the O stars, $0.002 \leq a_{\text{DAC}}R_{\star}/v_{\infty}^2 \leq 0.059$, while for the CSPN, we have $0.004 \leq a_{\text{DAC}}R_{\star}/v_{\infty}^2 \leq 0.071$, where the upper limit is 0.047 if we exclude IC 4593, for which the DAC progression is poorly constrained (see Fig. 3.). We conclude that the range of this parameter, which is related to CIRs, is similar for both CSPNe and OB stars, pointing to a common origin for both.

ACKNOWLEDGMENTS

D.L.M. acknowledges support from NASA's ADAP Grant NNX11AD28G. We are grateful for the comments of the referee.

REFERENCES

- Aerts C., Puls J., Godart M., Dupret, M.-A. 2009 *A&A*, 508, 409
 Balick B., Hajain A.R. 2004, *AJ*, 127, 2269
 Brown J.C., Barrett R.K., Oskinova L.M., Owocki S.P., Hamann W.-R., de Jong J.A., Kaper L., Henrichs H.F. 2004, *A&A*, 413, 959
 Cantiello M., Langer N., Brott I., de Koter A., Shore S.N., Vink J.S., Voegler A., Lennon D.J., Yoon S.-C., 2009, *A&A*, 499, 279
 Cranmer S.R., Owocki S.P. 1996, *ApJ*, 462, 469
 de Jong, J.A. et al. 2001, *A&A*, 368, 601
 De Marco O. 2009, *PASP*, 121, 316
 Donati J.-F., Semel M., Carter B.D.; Rees D.E., Collier Cameron A. 1997, *MNRAS* 291, 658
 Fullerton, A.W., Massa, D.L., Prinja, R.K., Owocki, S.P., Cranmer, S.R. 1997, *A&A*, 327, 699
 Fullerton A.W., Gies D.R., Bolton C.T. 1996, *ApJS*, 103, 475
 Georgiev L.N., Peimbert M., Hillier D.J., Richer M.G., Arrieta A., Peimbert A., 2008, *ApJ*, 681, 333
 Gray D.F., 1992, in *The observation and analysis of stellar photospheres*, *Camb. Astrophys. Ser.*, Vol. 20
 Guzmán, L., Loinard L., Gómez Y., Morisset C., 2009, *ApJ*, 138
 Handler G. 2003, *ASP Conf. Ser.*, 292, p. 183
 Hubeny I., Lanz T. 1995, *ApJ*, 439, 875
 Kaper L. et al. 1997, *A&AS*, 327, 281
 Kaper L., Henrichs H.F., Nichols J.S., Telting, J.H. 1999, *A&A*, 344, 231
 Kudritzki R.P., Urbaneja M.A., Puls J. 2006, *IAU Symp.* 234, 'Planetary Nebulae in our Galaxy and Beyond', eds. M.J. Barlow & R.H. Mendez, CUP, 119.
 Lamers H.J.G.L.M., Cerrutti-Sola M., Perinotto M. 1987, *ApJ*, 314, 726
 Langer N., Heger A., Wellstein S., Woosley S.E. 1999, *A&A*, 346, L37
 Lobel A., Blomme R. 2005, *ApJ*, 678, 408
 Markova N., Puls J., Repolust T., Markov H. 2004, *A&A*, 413, 693

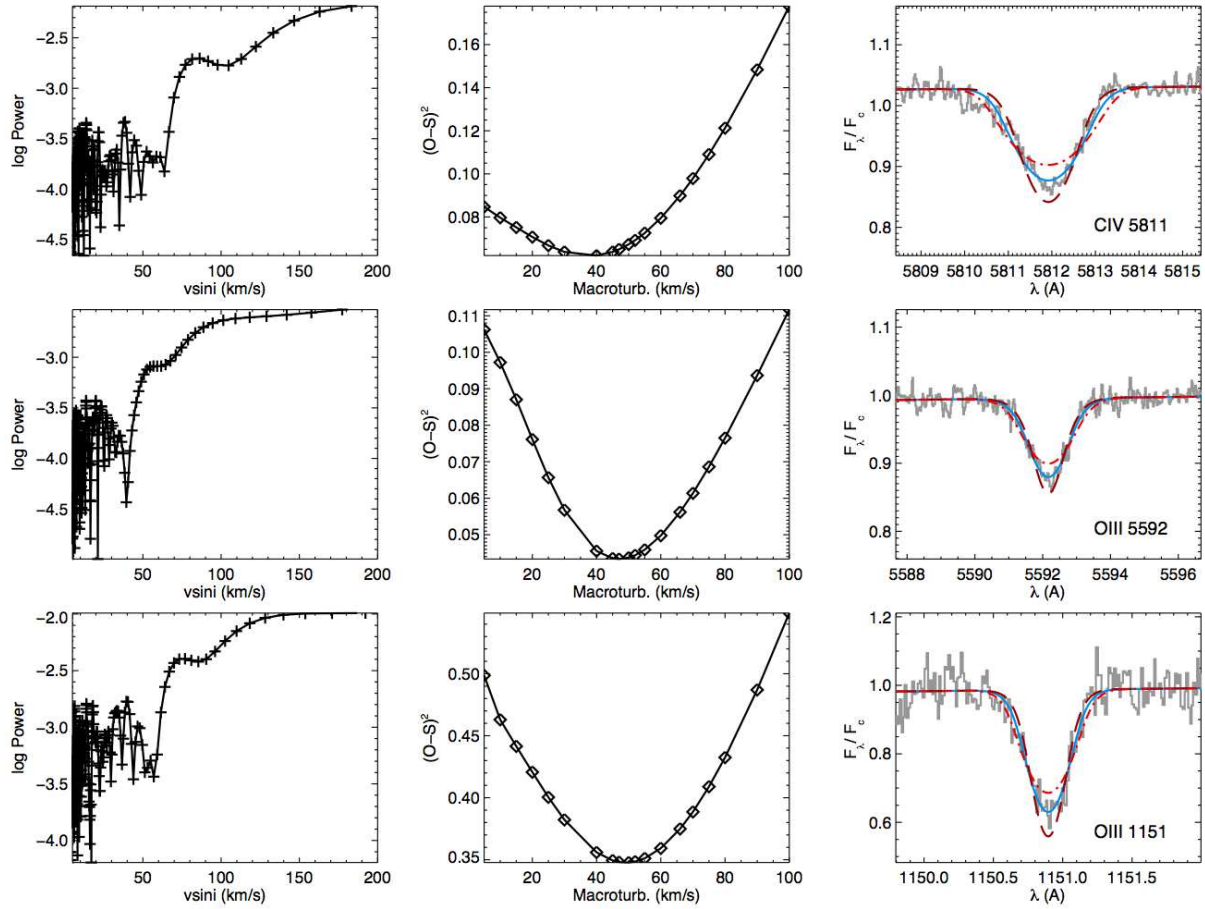


Figure 5. Determination of the projected rotational velocity for the representative case of IC2149 based on UV and optical spectra lines. For each line, the first panel shows the FFT determination of $v \sin i$; the second panel displays the determination of the macroturbulence velocity, whilst the third panel shows a comparison of the observed (grey) and theoretical profile (solid) convolved with a rotational profile characterized by the derived $v \sin i$ and with a radial-tangential macroturbulence profile defined by the macroturbulence velocity. Two other synthetic profiles, convolved with rotational profiles for $v \sin i \pm 15$ km/s, are also shown (dashed, dot-dashed).

Table 4. Comparison of normalised DAC accelerations for CSPN and O stars.

Star	R_\star/R_\odot	v_∞ (km s $^{-1}$)	$v \sin i$ (km/s)	a_{DAC} (km s $^{-2}$)	$a_{\text{DAC}} R_\star/v_\infty^2$	$v \sin i/v_\infty$
68 Cyg	16	2500	300	0.0200	0.0343	0.118
ξ Per	14	2450	220	0.0170	0.0276	0.090
λ Cep	21	2250	200	0.0140	0.0406	0.089
ζ Ori	22	2100	124	0.0170	0.0590	0.059
19 Cep	23	2050	100	0.0007	0.0028	0.049
λ Ori	15	2400	66	0.0011	0.0020	0.028
15 Mon	9	2000	67	0.0025	0.0039	0.034
10 Lac	8	1200	30	0.0018	0.0070	0.025
NGC 6826	2	1200	50	0.0530	0.0457	0.042
IC 418	2	700	56	0.0160	0.0466	0.080
IC 4593	2	950	55	0.0420	0.0706	0.058
IC 2149	4	1000	54	0.0090	0.0242	0.054
NGC 6543	1	1400	85	0.0220	0.0044	0.061

The O star DAC accelerations (a_{DAC}) are derived from Kaper et al. (1999). The O star parameters are from Repolust et al. (2004), Markova et al. (2004), Martins et al. (2005) and Simón-Díaz et al. (2006). We assign a $\pm 25\%$ propagated error for the normalised accelerations ($a_{\text{DAC}} R_\star/v_\infty^2$).

- Martins F., Schaerer D., Hillier D.J. 2005, *A&A*, 436, 1049
Massa, D., et al. 1995, *ApJL*, 452, 53
Massa, D., Fullerton, A.W., Sonneborn, G., Hutchings, J.B. 2003, *ApJ*, 586, 996
Morisset C., Georgiev L. 2009, *A&A*, 507, 1517
Muijres L.E., de Koter A., Vink J.S., Krticka J., Kubat J., Langer, N. 2011, *A&A*, 526, 32
Patriarchi P., Perinotto M. 1995, *A&AS*, 110, 353
Patriarchi P., Perinotto M. 1997, *A&AS*, 126, 385
Prinja R.K. 1988, *MNRAS*, 231, 21P
Prinja R.K., Massa D., Fullerton A.W. 2002, *A&A*, 388, 587
Prinja R.K., Hodges S.E., Massa D.L., Fullerton A.W., Burnley A.W. 2007, *MNRAS*, 382, 299
Prinja R.K., Massa D.L. 2010, *A&A*, 521, 55
Repolust T., Puls J., Herrero A. 2004, *A&A*, 415, 349
Simón-Díaz S., Herrero A. 2007, *A&A*, 468, 1063
Simón-Díaz S., Herrero A., Esteban C., Najarro F. 2006, *A&A*, 448, 351
Simón-Díaz S., Herrero A., Uytterhoeven K., Castro N., Aerts C., Puls, J. 2010, *ApJ*, 720, L174
Stanghellini L. Shaw R.A., Villaver E. 2008, *ApJ*, 689, 194
Suijs M.P.L., Langer N., Poelarends A.-J., Yoon S.-C., Heger, A., Herwig, F. 2008, *A&A*, 481, 87
Sundqvist J.O., Puls J., Feldmeier A., *A&A*, 510, 11

This paper has been typeset from a \TeX / \LaTeX file prepared by the author.